LA-UR-93-0004

Title: SPECTROSCOPIC EFFECTS OF DISORDER AND VIBRATIONAL LOCALIZATION IN MIXED-HALIDE METAL-HALIDE CHAIN SOLIDS

LA-UR--93-0004

DE93 007361

Author(s): Steven P. Love, Brian Scott, L. A. Worl, S. C. Huckett, A., Saxena, X. H. Huang, A. R. Bishop and Basil I. Swanson

Submitted to: Non-Linear Optical Materials of Advanced Materials
SPIE Conference # 1857
Los Angeles Airport Hilton Hotel
Los Angeles, California
January 16 - 23, 1993

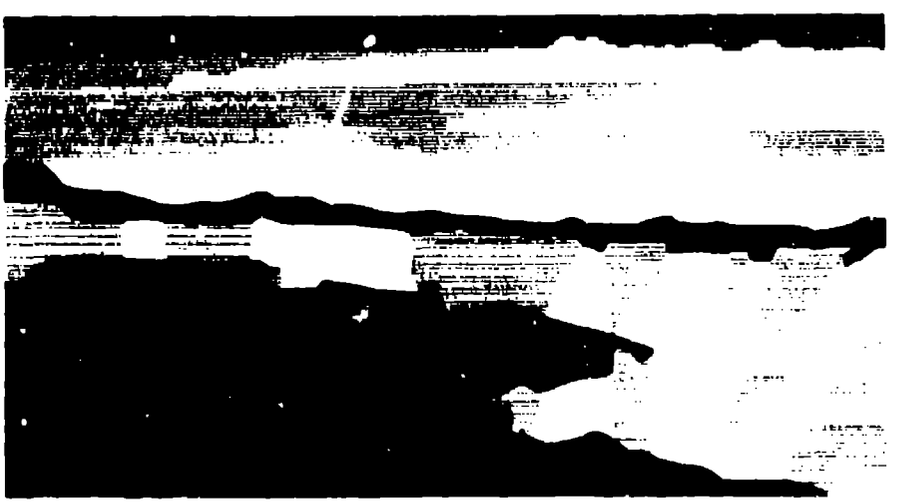

Los Alamos
NATIONAL LABORATORY

Spectroscopic effects of disorder and vibrational localization in mixed-halide metal-halide chain solids

S. P. Love,[1] B. Scott,[1] L. A. Worl,[1] S. C. Huckett,[1] A. Saxena,[2]
X. Z. Huang,[2] A. R. Bishop[2] and B. I. Swanson[1]
[1]Spectroscopy Group (INC-14) and [2]Theoretical Division (T-11)
Los Alamos National Laboratory, Los Alamos, NM 87545

ABSTRACT

Resonance Raman techniques, together with lattice-dynamics and Peierls-Hubbard modelling, are used to explore the electronic and vibrational dynamics of the quasi-one-dimensional metal-halogen chain solids $[Pt(en)_2][Pt(en)_2X_2](ClO_4)_4$, (en = $C_2H_8N_2$ and X=Cl, Br), abbreviated "PtX." The mixed-halide materials $PtCl_{1-x}Br_x$ and $PtCl_{1-x}I_x$ consist of long mixed chains with heterojunctions between segments of the two constituent materials. Thus, in addition to providing mesoscale modulation of the chain electronic states, they serve as prototypes for elucidating the properties to be expected for macroscopic heterojunctions of these highly non-linear materials. Once a detailed understanding of the various local vibrational modes occurring in these disordered solids is developed, the electronic structure of the chain segments and junctions can be probed by tuning the Raman excitation through their various electronic resonances.

1. INTRODUCTION

The halogen-bridged mixed-valence transition metal chain complexes, or "MX chain solids" consist of weakly interacting one-dimensional chains of alternating metal(M) and halide(X) atoms, held together by a ligand-counterion network, which can take on a variety of broken-symmetry ground states (charge density wave, spin density wave, etc.) that can be tuned by varying the chemical composition. In terms of potential applications, the MX materials display strong optical nonlinearities , as well as photo-induced charge separation at heterojunctions. But the primary interest in these materials lies in the realm of fundamental physics, because they serve as model systems for understanding a wide variety of low-dimensional phenomena relevant to such materials as conducting polymers and cuprate superconductors. Because of their relative simplicity, their crystalline nature and the associated simplicity of interpreting optical spectra, and the ability to chemically tune to the phase boundary between competing ground states, the MX materials make ideal test cases for exploring the validity various theoretical approaches.[1]

Solids of the form $[Pt(en)_2][Pt(en)_2X_2](ClO_4)_4$, (en = 1,2-diaminoethane and X=Cl, Br, or I), generally referred to by the abbreviations "PtX," are the most widely studied members of the MX class. These materials display a commensurate charge density wave (CDW) on the metals (i.e. the Pt ions are in alternating valence states $Pt^{III+\delta}$ and $Pt^{III-\delta}$, with δ large (~1) for PtCl and small for PtI), an accompanying Peierls distortion of the halide sub-lattice, and an intense, highly anisotropic optical absorption associated with the metal-metal intervalence charge transfer (IVCT) gap. The work described here is aimed at elucicating the nature of junctions formed between chains made with a single metal species but differing halides, i.e., between PtX and PtX' chains. Questions which arise regarding such junctions include the spatial extent of the transition region from one electronic structure (CDW strength, etc.) to another, and whether charge injection from one material to another occurs, as in metal-semiconductor Schottky junctions. While macroscopic PtX/PtX' heterojunctions have proved difficult to fabricate, microscopic collections of these junctions form naturally in $PtX_{1-x}X'_x$ mixed solids. Furthermore, the nanoscale modulation of properties which occurs in these mixed materials is of interest in itself. Optical studies, in particular resonance Raman (RR) measurements, are particularly powerful tools for characterizing these quasi-1-D mixed materials; with RR is possible to tune the Raman excitation into resonance with the

electronic transitions of particular types of junctions and chain segments, and hence explore the electronic structure as it is reflected in the vibrational behavior. The basic problem with the mixed materials is that we now move into the realm of disordered solids, and the sometimes surprising consequences of disorder in 1-D on vibrational spectra must first be understood. Here we explore these effects, first for the simplest case of pure PtCl, where the disorder arises from randomly distributed Cl isotopes, then for the more drastic cases of the mixed-halide materials $PtCl_{1-x}Br_x$ and $PtCl_{1-x}I_x$, and finally use the results to infer the nature of the junctions and the perturbations of the segments in the mixed materials.

2. VIBRATIONAL CONSEQUENCES OF DISORDER IN ONE DIMENSION—AN OVERVIEW

The key to extracting useful information from the resonance Raman spectra of the MX or other quasi-1-D materials is to recognize and understand in detail the spectroscopic consequences of disorder in a one-dimensional lattice. Once these sometimes complex details — involving the disorder-induced production of localized vibrational modes — are quantitatively understood, the frequencies and resonance enhancement profiles of the various modes can be used to determine the various local environments responsible for these modes. Fortunately, for highly one-dimensional systems such as the MX materials, the effects of disorder are relatively easy to understand and interpret.

The effect of disorder on the vibrational properties of a solid is one of the classic problems of lattice dynamics. A traditional starting point for theoretical exploration of this problem has been the random two-component linear chain, in which the two components are treated as isotopes in the sense that they differ only in mass, with interatomic forces remaining identical. Early computer simulations on such systems yielded an intricate fine structure in the vibrational density of states, consisting of a multitude of sharp peaks, which surprisingly did not smooth out as the number of atoms in the simulation was increased, even when tens of thousands of atoms were used.[2,3] This ran counter to the intuitive notion that phonons, by their extended nature, should in effect see a long-range average over the two components to produce a relatively smooth spectrum. The physical explanation for this unexpected result was that the disorder led to vibrational modes which no longer can be considered extended phonons, but rather are localized on just a few atoms, and that the various peaks correspond to modes associated with highly probable sequences of the two components. As discussed below, our results for PtCl provide the first direct experimental confirmation of these predictions for a real quasi-one-dimensional solid.[4]

An intuitive understanding of the completely disordered chain can best be gained by approaching the problem in stages. The first stage is to consider a single defect, e.g. an atom of the wrong mass, in an otherwise perfect chain; one then obtains the familiar localized defect modes.[5] For a two-component chain with the defect atom substituting for the lighter component, these defect modes obey the following rule: if the substituted atom is lighter than the original, the defect mode must lie above the highest mode of the associated optic phonon branch, and if it is heavier, it must lie below the lowest phonon in that branch.[5] Thus the dispersion of the associated phonon branch plays a critical role in determining the frequency of the defect mode. (For mixed chains such as the PtBr/PtCl and PtI/PtCl systems, the junctions between long segments of the two types of chain can also be thought of as "defects," since the translational symmetry is broken at the junction, and there will be vibrational modes localized at the junctions.)

The second stage is to consider the effects of two such defects in an otherwise perfect chain. As before, we will get local modes at each defect. But in addition, the two defects now impose boundary conditions on the segment of chain between them. This leads to a new set of vibrational modes, distinct from the extended phonons and the defect local modes, localized on this chain segment. Depending on the degree of mismatch between the defect and the rest of the lattice, and the ordinary phonon spectrum of the lattice, these segment modes can take two basic forms.

In the simpler type, the vibrational amplitude does not extend significantly into the lattice beyond the two defects, or even to the defects themselves, but is localized amost entirely on the segment. For this type of segment mode, which dominates in the $PtCl_{1-x}Br_x$ system discussed below, the segment modes with substantial IR or Raman activity will be those without any nodes within the segment. A first approximation for the frequency to be expected for such modes can

be obtained by noting that the atomic displacement pattern of such a mode is quite similar to a piece of a of non-zero wavevector phonon from the associated branch; a segment mode localized on a segment of length d will correspond approximately to a phonon of wavevector π/d. Hence, as was the case for the defect local mode, the dispersion of the associated phonon branch for the perfect chain plays a major role in determining the frequencies of these segment modes.

For this simpler type of segment mode, the frequencies of the segment modes do not depend strongly on the nature of the defects defining the segments. Thus, for example photo-induced electronic defects like polarons and bipolarons, which would be manifested as force constant defects, could also lead to segment modes very similar to those formed by mass defects, as long as the electronic defect is strongly localized and occurs in sufficiently high numbers.

In the second type of segment mode, two defects still define a segment, but the vibrational amplitude penetrates a significant distance into the lattice beyond the defects, so that the segment, the defects, and a bit of the surrounding lattice all participate in the local mode. This less strongly localized type of segment mode can occur when the mismatch between the defect and the rest of the lattice is small, when the defect modes are in resonance with a lattice phonon band, or when the electronic structure changes gradually rather than abruptly near the defects. These weakly localized segment modes are prominent in the $PtCl_{1-x}I_x$ system, and lead to extremely complex resonance Raman behavior.

The case of a completely random mixed chain is essentially a combination of several of the above effects. For severe enough disorder (large enough mass differences between the mixed components), the vibrational modes are so strongly localized that each segment or defect feels only the effects of its immediate neighborhood, and acts as if it were an isolated segment in a long chain of the type defined by that immediate neighborhood. The observed vibrational spectrum will then be just a few localized modes residing on the segments and defects which occur with the highest probability. (For weaker localization, the length of the relevant segments, and hence and the number of possible types of segment, becomes larger, so that a large number of modes will occur, eventually merging into a broad band.) The particularly simple form taken by the localized modes in 1-D, and their strong dependence on the dispersion of the associated phonon branches, suggests that phonon dispersions can be extracted from an analysis of the local mode frequencies. As will be seen below, this provides a novel way of obtaining phonon dispersion information by purely optical means, a measurement which is impossible in perfect crystals (inelastic neutron scattering is the primary method) due to the crystal momentum conservation selection rule ($\Delta q = 0$) operant in both IR and Raman spectroscopy.

3. LOCALIZATION BY CHLORIDE ISOTOPIC DISORDER IN PtCl

The spectral complexity which can arise from purely isotopic disorder, with no electronic defects, is illustrated by the pure PtCl system. Figure 1 shows the Raman and infrared spectra of PtCl at roughly 20K for the fundamental $Cl\text{-}Pt^{III+\delta}\text{-}Cl$ symmetric stretch (ν_1) and asymmetric stretch (ν_2) phonon regions. Shown on top are spectra for samples prepared with natural Cl isotope abundance (75% ^{35}Cl, 25% ^{37}Cl); on the bottom are spectra for samples prepared with ~99% pure ^{35}Cl. Clearly the fine structure seen in the top spectra arises from Cl isotopes, but there are several puzzling aspects. Why, for instance, is the ν_1 Raman fine structure so complex compared to the simple three-peaked structure seen in the IR for ν_2? And how does the addition of *heavier* isotopes lead to ν_1 fine structure components *higher* in frequency than for the pure ^{35}Cl case?

All these surprising features are purely lattice dynamical in origin, and can be understood in terms a simple 1-D harmonic mass-and-spring model. Figure 2 shows simulated Raman[4] and IR[6] spectra, obtained from such a model which included only Pt and Cl atoms with first- and second-nearest neighbor interactions. Comparison with Fig. 1 reveals remarkably good agreement. To produce these simulated spectra, the model spring constants were first obtained by fitting the model to the ~99% ^{35}Cl case. This fit included the weak satellite peaks in the experimental spectra, arising from the localized modes of isolated ^{37}Cl "defects;" doing so defined the phonon dispersions for the ν_1 and ν_2 branches. The eigenfrequencies and eigenvectors were then obtained for a hundred 128 atom chains having randomly distributed ^{35}Cl and ^{37}Cl. The Raman cross-sections and IR dipole moments were calculated for each eigenvector, and the results combined to form the simulated spectra.[4,6]

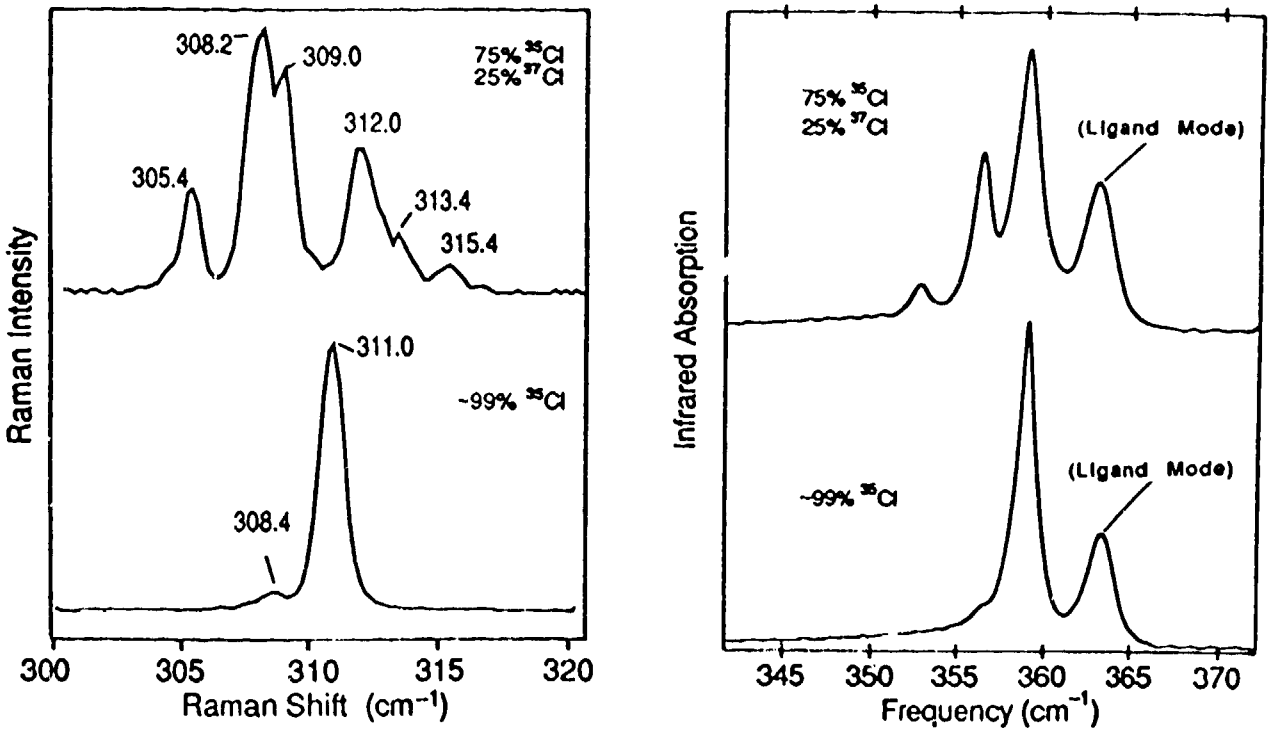

Fig. 1. Experimental Raman and infrared spectra of PtCl at approximately 15 K, for natural Cl isotopic abundance (top) and for ~99% isotopically pure ^{35}Cl (bottom). (after Refs. 4 & 6)

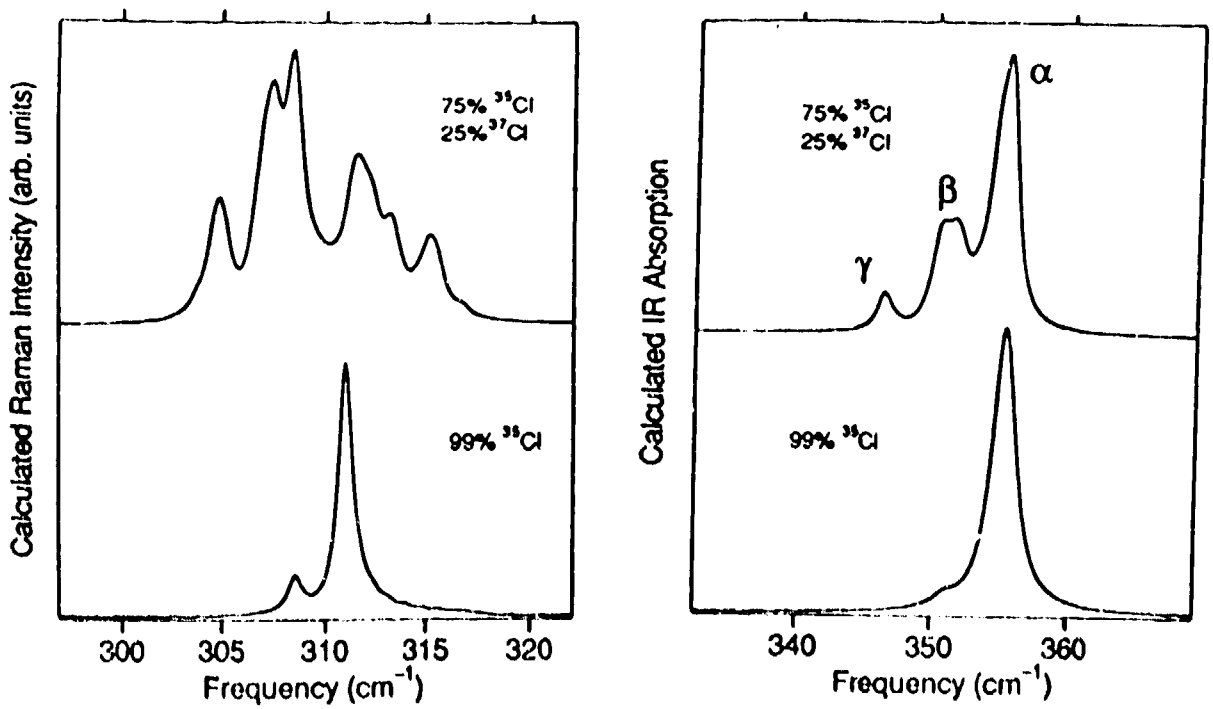

Fig. 2. Raman and infrared spectra of PtCl calculated from the harmonic linear chain model, for natural Cl isotopic abundance (top) and for 99% isotopically pure ^{35}Cl (bottom). (after Refs. 4 & 6)

The model shows that the unusual features of these spectra are a consequence of the surprising fact that even the small mass difference (~5%) between the two randomly distributed Cl isotopes is a severe enough disruption of translational symmetry to put the vibrational modes into the strongly localized regime. As predicted for this case in the previous section, the observed modes are found to reside on short chain segments defined by a few statistically favored sequences of isotopes. Figure 3 shows the isotope sequences and approximate eigenvectors for the six strongest observed Raman peaks; the same isotope sequences give rise to the IR modes.

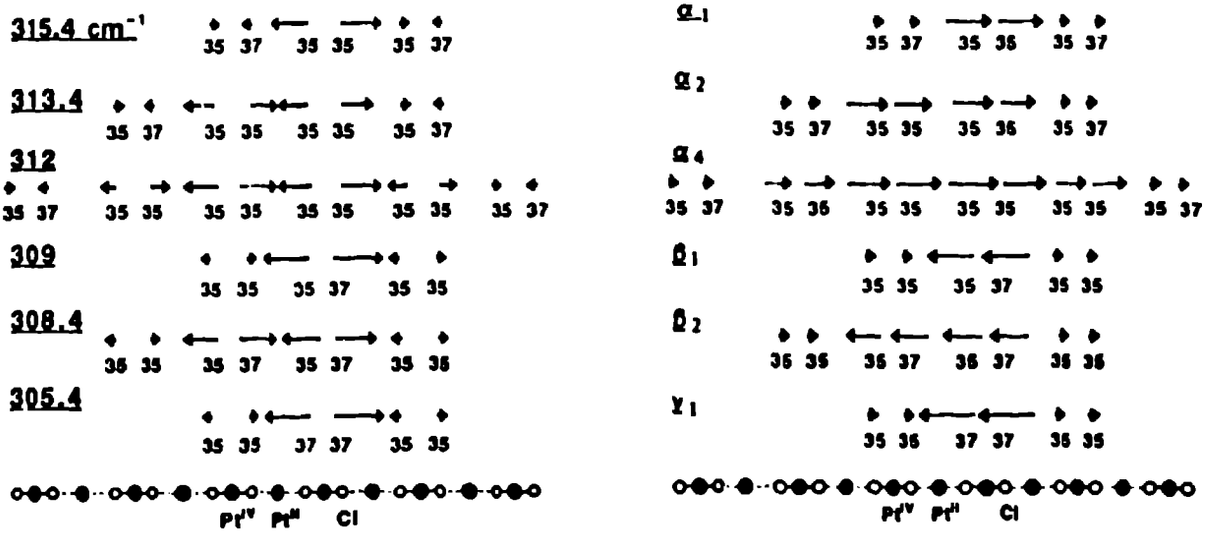

Fig. 3. Cl isotope sequences and approximate atomic displacement eigenvectors for the six strongest Raman (left) and IR (right) localized modes in natural abundance PtCl. For clarity, only Cl displacements are shown. Frequencies for the Raman modes are shown. For the IR, modes labelled α, β, and γ fall within the frequency ranges of the correspondingly labelled features in Fig. 2.

The remarkably different appearances of the observed fine structures for the Raman-active ν_1 mode and the IR-active ν_2 mode are found to be the result of different magnitudes and directions of dispersion for the two phonon branches, with the ν_1 frequency of the isotopically pure material increasing with increasing phonon wavevector by 6.5 cm^{-1} from Brillouin zone center (Γ) to zone boundary (X), while ν_2 disperses downward by less than 3 cm^{-1}. Given the upward dispersion of the ν_1 branch, the ordering of the modes, with shorter segments corresponding to higher frequency, makes intuitive sense. The question of how adding heavier isotopes can produce higher frequency ν_1 components is also answered: the heavy atoms act to define short segments of light-isotope chain, which for upward dispersion have modes higher in frequency than the zone center (infinite chain) phonon. For the ν_2 branch, the dispersion is so small that the local modes for all segment lengths cluster closely around the frequencies for ordered ^{35}Cl-Pt^{IV}-^{35}Cl---Pt^{II}, ^{37}Cl-Pt^{IV}-^{35}Cl---Pt^{II}, and ^{37}Cl-Pt^{IV}-^{37}Cl---Pt^{II} chains.[6]

4. LOCALIZED MODES IN THE $PtBr_{1-x}Cl_x$ SYSTEM

Compared to pure PtX systems containing a single halide species, the resonance Raman spectra of mixed-halide systems, shown in Fig. 4, are strikingly rich and complex, displaying a multitude of puzzling features not seen in either of the constituent pure PtX materials.[7] The Raman spectra of pure PtCl or PtBr are dominated by the fundamental

$X-Pt^{IV}-X$ symmetric stretch (ν_1) chain phonon, at 308 or 165.5 cm^{-1}, respectively, which are dramatically enhanced when the excitation energy is near resonance with the IVCT band. In contrast, for the mixed $PtBr_{1-x}Cl_x$ system the 165.5 cm^{-1} mode is replaced a series of lines between 181 and 166 cm^{-1}, each coming into resonance at successively lower excitation energies, so that typically two or three neighboring lines are observed at a given excitation energy, producing an apparent Raman "dispersion".[8] In addition there appears a cluster of modes near 210 cm^{-1} which also show strong excitation dependence, and another cluster near 324 cm^{-1} which are both Raman- and infrared-active.

A systematic spectroscopic study of the $PtBr_{1-x}Cl_x$ system has enabled us to determine that the mechanism for the complex spectral behavior of this system is closely related to that responsible for the isotopic fine structure in pure PtCl, again involving vibrational modes localized on finite segments, this time defined by sequences of Cl and Br rather than by isotopes. The $PtBr_{1-x}Cl_x$ case has the added complication that the PtBr and PtCl segments have different electronic properties, leading to different excitation profiles for the various segments, thus necessitating a more detailed theoretical treatment than for the Cl isotope problem.

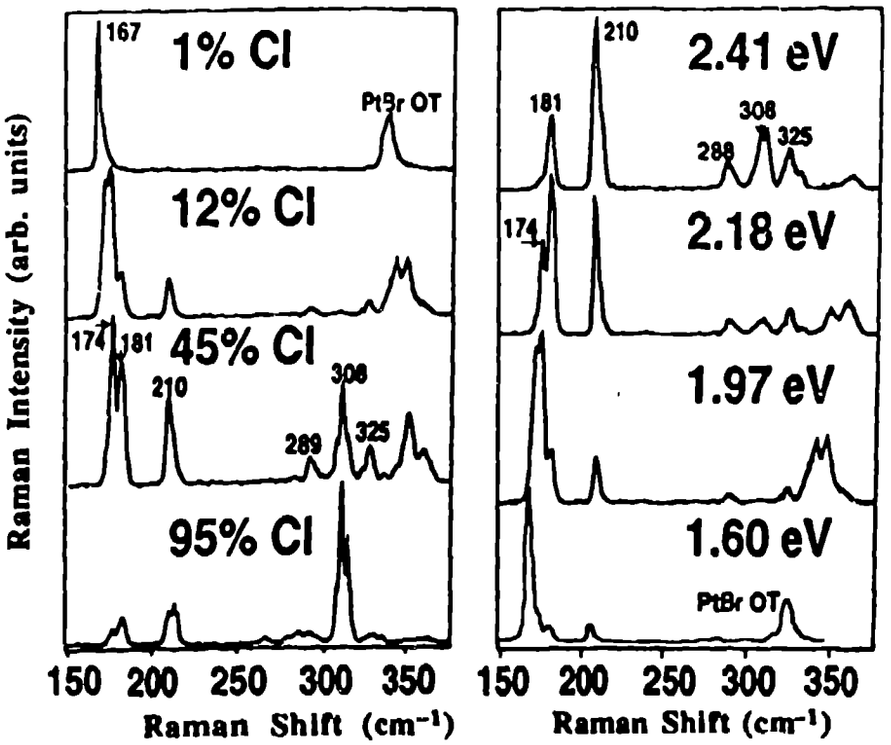

Fig. 4. (Left) Cl concentration (x) dependence of Resonance Raman (RR) spectra at 1.98eV for $PtCl_xBr_{1-x}$ crystals. (Right) Excitation dependence of RR spectra of $PtCl_{0.12}Br_{0.88}$. (after Ref. 9)

The frequencies of all the observed features, as well as their composition dependence and excitation profiles, can be accurately predicted in a 3/4-filled two-band Peierls-Hubbard treatment[9] in which the mixed chain consists of interspersed short segments of pure PtBr and PtCl. An important prediction of this model is that the electronic healing length between the PtBr and PtCl segments is very short, so that the interatomic force constants within the short segments are essentially the same as in the corresponding pure material. Thus, vibrationally, we are again in a situation very similar to that of the Cl isotopes of the previous section, but with the disorder much more drastic. The 181–166 cm^{-1} series arises from the ν_1 mode of successively longer segments of PtBr embedded in PtCl, with the 181 cm^{-1} mode corresponding to a single $Br-Pt^{IV}-Br$ unit. A comparison of theoretically predicted and observed frequencies for these segment modes is shown in

Fig. 5. The ~210 cm^{-1} and the ~324 cm^{-1} modes arise whenever a PtBr / PtCl junction occurs at a Pt^{IV} site, and correspond to the stretching modes of the Br–Pt^{IV}–Cl unit thus formed, with their exact frequencies depending weakly on the lengths of the associated segments. As in the first section, the eigenvectors for the segment modes of the 181–166 cm^{-1} series closely approximate PtBr ν_1 phonons of various wavevectors. Thus the mixed system results enable us again to indirectly infer the dispersion of this phonon branch as being upward from Γ to X by roughly 50 cm^{-1}. Further, the excellent agreement between the experiment and the model confirms the model's prediction of a very short electronic healing length at the PtCl/PtBr junctions; were this not the case, the vibrational spectrum would be drastically different, as with the $PtCl_{1-x}I_x$ case below.

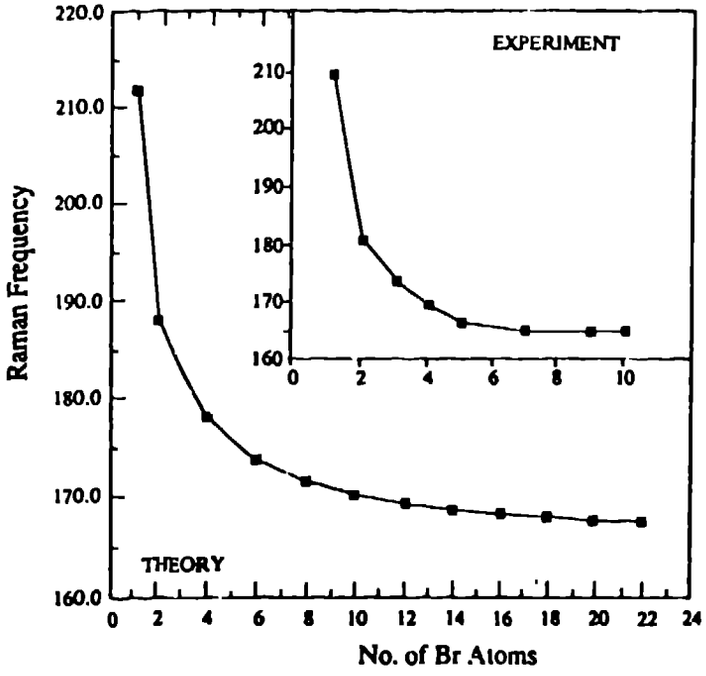

Fig. 5. Calculated and experimental Raman mode frequency as a function of PtBr segment length, including the 210 cm^{-1} junction mode. (after Ref. 9)

5. THE $PtCl_{1-x}I_x$ SYSTEM

Resonance Raman spectra of materials in the $PtCl_{1-x}I_x$ system are distinguished by being considerably more complex than those of $PtCl_{1-x}Br_x$ materials. Space does not permit a complete discussion of the experimental and theoretical work on these materials. Here we summarize some of the more important results. Raman spectra at some representative excitation energies for the case where x=0.2 are shown in Fig. 6, together with those of pure PtCl and pure PtI for comparison. Among the notable features of the $PtCl_{1-x}I_x$ spectra are the cluster of modes between 149 and 176 cm^{-1}, another cluster between roughly 260 and 290 cm^{-1}. Also apparent are modes in the 300 cm^{-1} region, which Cl-isotope enrichment experiments show are purely PtCl-like in character but are shifted downward significantly from the pure PtCl value, and modes from roughly 130 to 145 cm^{-1} which the isotope studies show are purely PtI-like but which lie far above the pure PtI frequency. Not shown in Fig. 6 are the various overtones and combination bands which occur; most notable is the fact that lines in the 149-176 cm^{-1} series form combination bands with the ~260-290 cm^{-1} series (i.e. features appear at 176+263, etc.), and also that both series form combinations with the ~300 cm^{-1} PtCl modes. The implication of these combination bands is that the 149-176 and ~260-290 cm^{-1} series arise from either the same microscopic objects (chain segments, junctions, etc.), or from objects which are physically connected on an atomic scale, and further that these objects are closely associated with relatively long PtCl chain segments.

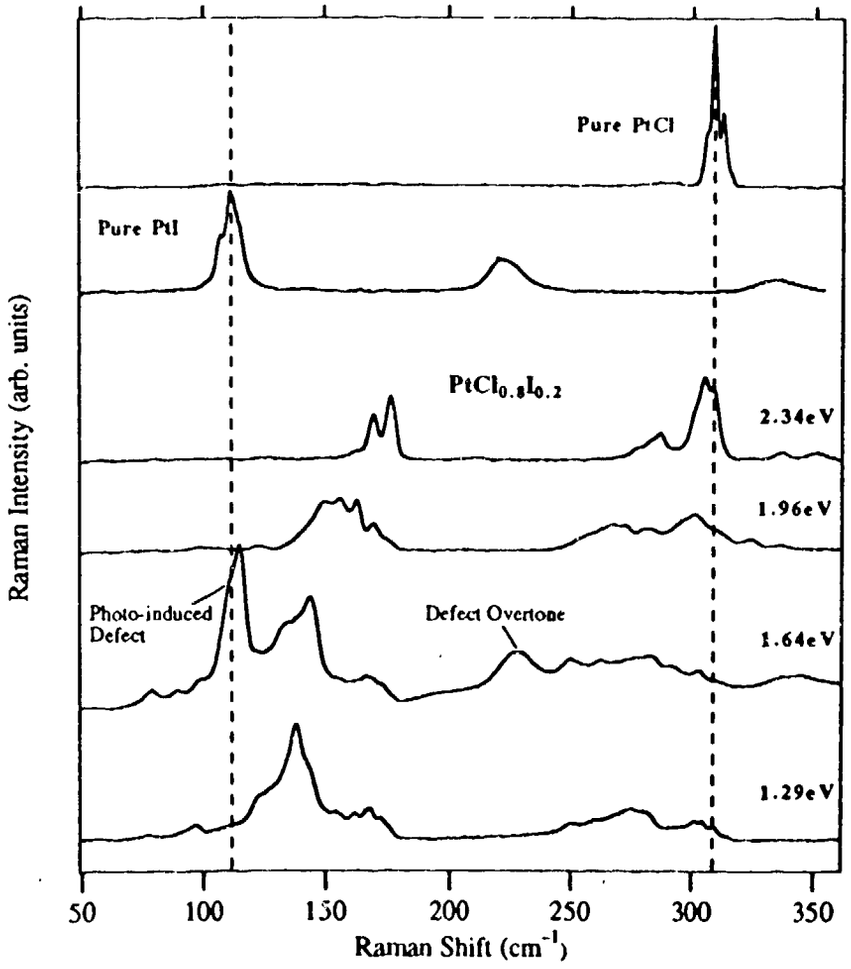

Fig. 6. Resonance Raman spectra of $PtCl_{0.8}I_{0.2}$ at 15 K for various excitation energies indicated on the right. Also shown, for comparison, are Raman spectra for pure PtCl (excitation energy 1.6 eV) and pure PtI (excitation energy 1.28eV).

Given these combination bands, a reasonable guess for the origin of the 149-176 and ~260-290 cm^{-1} series would be that they are junction modes analogous to the ~210 and ~324 cm^{-1} modes of $PtCl_{1-x}Br_x$. But harmonic lattice dynamics demands that the upper modes should be above 305 cm^{-1}; also, lattice dynamics does not predict junction modes spread over such a wide frequency range. More detailed Peierls-Hubbard modelling shows that the harmonic approximation breaks down badly for PtI. The Peierls-Hubbard modelling gives the correct origin of these features: The 149-176 cm^{-1} series arises from various short PtI segments. The ~260-290 cm^{-1} series arises from segment modes of the second type discussed in Section 2, in which PtCl segments are defined by the short PtI segments responsible for the 149-176 cm^{-1} series, but for which the vibrational amplitude extends to include central PtCl segment, the PtI segments, and some of the PtCl beyond. This interpretation is supported by the Cl isotope substitution experiments which show that these modes have strongly mixed PtCl and PtI character.

The softening of the ~300 cm^{-1} PtCl-like modes compared to pure PtCl occurs despite two effects which normally would increase the observed frequency. The first of these this the division of the PtCl chain into segments separated by PtI. As discussed in the previous sections, the dispersion of the Raman-active phonon is upward from Brillouin zone center to zone boundary, so chain cutting should result in segment modes of higher frequency, by a few cm^{-1}, than the

q=0 PtCl phonon. The second effect is implied by x-ray structural studies, which show that the Pt-Pt separation in the PtCl segments of $PtCl_{1-x}I_x$ is larger than in pure PtCl, a condition which ordinarily strengthens the CDW and hence stiffens the ν_1 frequency. The fact the observed ν_1 frequency actually is lower than in pure PtCl implies that there is a strong softening effect which counteracts these other two effects. Peierls-Hubbard modelling shows this softening arises because the electronic healing length between PtI and PtCl is very long (many unit cells), hence this effect is in essence the weak CDW of PtI penetrating far across the PtI/PtCl junction into the normally strong CDW PtCl segments.

These experimental resonance Raman results have enabled us to determine which of two possible theoretical scenarios actually occurs in $PtCl_{1-x}I_x$. The first of these predicts that the large electronic band mismatch between PtCl and PtI, with the top of the PtI valence band falling above the PtCl conduction band, would result in the injection of electrons from the PtI segments into the PtCl in a manner similar to the formation of a Schottky barrier at metal/semiconductor interfaces. The second possible scenario predicts that in assembling the mixed solid, the electronic bands would be perturbed, essentially by an additive constant, so that this charge injection would not occur. We find that this second scenario accurately predicts the obseved resonance Raman behavior while the first fails. In particular, with the parameters which allow charge injection, the model fails to predict the existence of the ~260-290 cm^{-1} series of modes.

6. CONCLUSIONS

We have seen in the PtCl Cl-isotope case and the $PtBr_{1-x}Cl_x$ and $PtCl_{1-x}I_x$ cases the general result that disorder within the chain leads to vibrational modes localized on finite chain segments and at the junctions between segments, with the vibrational spectra dominated by modes associated with a few statistically favored types of segments. The simplicity of the 1-D case makes it possible to extract phonon dispersions through analysis of the disorder-induced fine structure. Furthermore, detailed understanding of the behavior of the various local modes has made it possible to test theories of the electronic structure of these materials. This has made it possibe to demonstrate experimentally that the electronic healing length between PtCl and PtBr is very short while it is quite long between PtCl and PtI, and that electron transfer from PtI to PtCl is negligible. Such approaches should be valuable for a wide variety of low-dimensional materials.

ACKNOWLEDGEMENTS

We thank A. D. F. Bulou and R. J. Donohoe for valuable discussions. Supported by the US DOE Office of Basic Energy Sciences, Materials Science Division, and the Center for Materials Science at Los Alamos National Laboratory.

REFERENCES

1. J. T. Gammel, A. Saxaena, I. Batistic´, A. R. Bishop, and S. R. Phillpot, Phys. Rev. B 45, 6408 (1992); S. M. Weber-Milbrodt, J. T. Gammel, A. R. Bishop, and E. Y. Loh, Phys. Rev. B 45, 6435 (1992), and references therein.
2. P. Dean, Proc. Roy. Soc. **A254**, 507 (1960); Proc. Roy. Soc. **A260**, 263 (1961).
3. W. M. Visscher and J. E. Gubernatis in *Dynamical Properties of Solids*, Vol. 4, edited by G. K. Horton and A. A. Maradudin, (North-Holland, Amsterdam, 1980).
4. S. P. Love, L. A. Worl, R. J. Donohoe, S. C. Huckett and B. I. Swanson, Phys. Rev. B **46**, 813 (1992).
5. A. S. Barker and A. J. Sievers, Rev. Mod. Phys. **47**, Suppl. No. 2 (1975).
6. S. P. Love, S. C. Huckett, L. A. Worl, T. M. Frankcom, S. A. Ekberg and B. I. Swanson, Phys. Rev. B, in press.
7. S. C. Huckett, R. J. Donohoe, L. A. Worl, A. D. F. Bulou, C. J. Burns, J. R. Laia, D. Carroll and B. I. Swanson, Chem. Mater. 3, 123 (1991).
8. R. J. H. Clark and M. Kurmoo, J. Chem. Soc., Faraday Trans. Series 2, **79**, 519 (1983).
9. X. Z. Huang, A. Saxena, A. R. Bishop, L. A. Worl, S. P. Love, and B. I Swanson, Solid State Commun. **84**, 951 (1992).